Catalysis Today 169 (2011) 138–149

Contents lists available at ScienceDirect

Catalysis Today

journal homepage: www.elsevier.com/locate/cattod

Preparation and characterization of catalysts based on oniumsilica-immobilized Keggin acids

T.V. Kovalchuk[a], H. Sfihi[b,c], V.N. Zaitsev[a], J. Fraissard[b,d,*]

[a] National T. Shevchenko University, Vladimirskaya 64, Kiev, Ukraine
[b] Laboratoire Photons et Matière, ESPCI, 10 rue Vauquelin, 75005 Paris, France
[c] Département de Physique, UFR SMBH, Université Paris 13, 74 rue Marcel Cachin, 93012 Bobigny Cedex, France
[d] University Pierre and Marie Curie, 4 place Jussieu, 75005 Paris, France

ARTICLE INFO

Article history:
Received 25 April 2010
Received in revised form 4 November 2010
Accepted 5 November 2010
Available online 3 January 2011

Keywords:
Keggin heteropolyacids
Acid onium salts
Surface-grafted cations
Oniumsilica-based HPA catalysts

ABSTRACT

A new method has been developed for preparing acid onium salts of Keggin heteropolyacids via ion exchange on amorphous silica functionalized with pyridinium and alkylimidazolium cations (SiO_2–Q). The interaction between HPA and the surface-grafted cations affords acid salts of HPA with intact Keggin structure. This method offers excellent dispersion of HPA on the surface and higher resistance to HPA leaching in polar media, compared to the silica-based materials. The solids are thermally stable up to 250–300 °C, depending on the onium cation and anion, the most stable being the samples with immobilized $H_4SiW_{12}O_4$ and $H_3PW_{12}O_{40}$.

1. Introduction

For the design of HPA-based heterogeneous acid catalysts several factors, such as the number of acid sites, their strength and accessibility to the reactants, must be considered. Moreover, for heterogeneous catalysts for liquid-phase reactions, hydrophobicity and stability towards leaching in polar media are required. With the aim of preparing new heterogeneous acid catalysts based on HPA and considering the above-mentioned factors, we immobilized HPA by electrostatic bonding to onium cations grafted on silica. This paper presents the synthesis procedure, structure and thermal stability of grafted HPA-onium salts. Their acidity and catalytic activity in ETBE synthesis and AcOH esterification with EtOH were reported elsewhere [1].

Salts of HPAs are classified in two groups depending on their solubility in water and other physicochemical properties [2–4]. The first group (denoted A) comprises the water-soluble salts of HPA and small cations (Li^+, Na^+). Their physicochemical properties resemble those of the parent HPAs: they have low surface area and low thermal stability [3,5]. The other group (denoted B) includes the salts formed by the larger cations, such as NH_4^+, K^+ and Cs^+. These salts are insoluble in water, and they can have a high surface area (up to 200 $m^2\,g^{-1}$) and microporosity [3,5]. B-Salts melt without decomposition, their stability being due to the stronger interaction of large heteropolyanions with large cations. A group of HPA salts formed by organic onium cations (R_4N^+, $R = C_nH_{2n+1}$) featuring high hydrophobicity and mesoporous structure has been reported by Stein et al. [6], Janauer et al. [7] and Taguchi et al. [8]. These salts are soluble in non-polar solvents, due to the lipophilic character of cation–anion associations. Increasing the cation size results in a weakening of the anion-anion and cation–anion interactions, as shown by the decrease in the M–O stretching frequencies in the HPA [9].

The acid strength of a solid acid is important in determining its activity in acid-catalysed reactions, but is not the only factor which governs the activity of many HPA-based catalysts [10]. Accessibility of the acid sites appears to be at least as important. In terms of the accessibility of acid sites, three types of solid HPA-based catalysts are generally considered [3]. In reactions with polar reactants, most generally accepted to proceed in the so-called "pseudo-liquid phase", bulk or silica-supported acids are highly active [3]. However, such catalysts have low accessibility for non-polar reactants, because the acid sites are situated in the bulk of the highly polar HPA phase. In solid B-group HPA salts most of the protons are superficial, so they are accessible to either type of reactant. For example, in alkylation reactions $Cs_{2.5}H_{0.5}PW_{12}O_{40}$ is more active than bulk HPAs [3]. The B-type salts display so-called "surface-type" or true heterogeneous catalysis [11].

* Corresponding author. Tel.: +33 0 1 49 11 19 48; fax: +33 0 1 46 02 19 62.
E-mail addresses: kovalchu@yahoo.com (T.V. Kovalchuk), hocine.sfihi@espci.fr (H. Sfihi), jacques.fraissard@upmc.fr, jacques.fraissard@club-internet.fr (J. Fraissard).

0920-5861/$ – see front matter © 2010 Elsevier B.V. All rights reserved.
doi:10.1016/j.cattod.2010.11.052

In view of the versatility of heteropolyanions as recyclable acid catalysts for liquid-phase applications, chemical grafting of HPA salts on siliceous supports seems attractive. We show here that such chemical immobilization can be readily achieved, for instance, by electrostatic interaction with grafted organic cations, such as onium cations. The large radii of these "soft" cations provide strong interaction with large "soft" HPA anions. Formally, these surface compounds can be regarded as B-group salts with several useful properties, such as accessibility of active sites, thermal stability and hydrophobicity to enhance the affinity towards non-polar reactants. The acidity of these materials may result from the inclusion of protons and the formation of acid salts. If acidity, availability of active centres and strong electrostatic retention of active anions are combined, the materials prepared in this way should exhibit catalytic activity in acid-catalysed reactions [1]. In addition, leaching of HPA can be nearly avoided to give reusable solids for liquid-phase catalysis.

The oniumsilica-based HPA materials, described in this paper, have not yet been reported in detail; they continue the research started in [12,16]. Related systems have been developed based on aminopropylated silica and Keggin ions for acid catalysis [12–15], or oniumsilica and polyoxometalates for liquid-phase oxidation catalysts [16]. Grafting approach, with the use of tetraethylammonium-, pyridinium- and *N*-methylimidazolium-silicas as supports, was described for the Lewis acids, $SnCl_4^-$ [17] and $AlCl_4^-$ [18]. In the same way as the so-called "ionic liquids" [18], grafted HPA anions are expected to have great mobility.

The salts of Keggin HPA were immobilized on silica in two steps. A large-pore precursor silica was treated to prepare grafted onium chlorides [19], which were exchanged with HPAs to produce the target salts. This paper focuses on preparation details and characterization of these materials: heteropolyanion distribution, which was studied by N_2 adsorption; their composition and structure, which were studied by elemental analysis, IR, NMR and UV–vis spectroscopies as well as their thermal stability, as needed for catalysis application.

2. Experimental

2.1. Catalyst preparation

Nomenclature

bulk HPAs: pure heteropolyacids in solid state
H_3A: anion of heteropolyacid (A) with three protons
-Q: grafted onium cation
-Q"H_2A": grafted HPA salt containing one onium cation and two residual protons
-Q_2"HA": grafted salt containing two onium cations and one residual proton
-Q_3"A": grafted neutral salt containing three onium cations and no protons
KU: Keggin unit
C_L: concentration of grafted ligand

Reagents. Heteropolyacids (HPA), $H_3PMo_{12}O_{40}{\cdot}nH_2O$ (denoted PMo), $H_3PW_{12}O_{40}{\cdot}nH_2O$ (PW), $H_4SiMo_{12}O_{40}{\cdot}nH_2O$ (SiMo) and $H_4SiW_{12}O_{40}{\cdot}nH_2O$ (SiW), reagent grade, were purchased from Fluka or Aldrich and purified by the Dreksel method (etherate extraction).

Grafted silica supports used. γ-Pyridiniopropylsilica (two different types: Py-1 and Py-2), γ-(N,N′-methylimidazolio)propylsilica (MeIm), γ-(N,N′-butylimidazolio)propylsilica (BuIm) (see Section 3.2).

Immobilization of Keggin acids. Oniumsilica and HPAs (PW, SiW) were activated in vacuum at 150 °C for 4 h (silica) and at 80 °C for 2 h (HPAs), respectively. To maintain the solubility in organic solvents and prevent reduction, no vacuum treatment was applied in the case of PMo and SiMo. A mixture of oniumsilica (2 g) and 10 ml of a *ca.* 0.1 M solution of HPAs (in MeCN for Py-1 and Py-2 and EtOH for MeIm and BuIm) was refluxed for 4–6 h, the solid separated by decantation, washed with the corresponding solvent and the exchange procedure repeated twice with fresh HPA solution. The catalysts prepared were washed in a Soxhlet apparatus with MeCN or EtOH for at least 12 h until physically adsorbed acid was completely removed. Analysis showed some initial leaching of HPA during the first 0.5–1 h of the hot wash (this will be discussed later). Though the HPA loss did not continue any further, the 12 h-wash was used for the preparation of all samples, to minimize their possible subsequent leaching in the course of the catalysis reactions. Samples were dried under vacuum at 80 °C for 4–6 h. They are denoted according to the precursor support and the HPA used for their preparation: for example, the Py-1-PW catalyst consists of support γ-pyridiniopropylsilica (Py-1) exchanged with $H_3PW_{12}O_{40}$ (PW). Therefore the prepared samples are denoted as follows (all samples are listed): Py-1-PW, Py-1-PMo, Py-1-SiW, Py-2-PW, Py-2-PMo, Py-2-SiW, MeIm-PW, MeIm-PMo, MeIm-SiMo, BuIm-PW, BuIm-PMo, BuIm-SiMo.

The onium salts of polyoxometalates prepared in this way are water-insoluble. After the extraction step and removal of physically adsorbed acid, no leaching of HPA occurs in either the organic solvents or water. Since no special precautions were taken to store the samples, they were reactivated before characterization, as indicated in each case.

Elemental analysis was used to determine the concentrations of HPA and grafted organic functions. Mo and W contents were determined by X-ray fluorescence spectroscopy for the samples diluted with H_3BO_3 (and, if needed, with silica) and pressed in pellets of controlled widths and surface, by comparison of the data with a calibration set prepared with known concentrations of HPA and silica.

2.2. Spectroscopies

Infrared spectroscopy. DRIFT spectra with *in situ* thermal study were recorded on a Bruker Vector 22 spectrometer equipped with a Harrick diffuse reflectance cell, DTGS detector (400 scans, resolution 4 cm^{-1}, KBr background). Samples were diluted 1:10 with KBr, ground into fine powders and put in the reaction chamber without pressing.

NMR spectroscopy. ^{31}P Single pulse excitation (SPE) and magic angle spinning (MAS) NMR measurements were performed at 202.47 MHz with a Bruker ASX 500 NMR spectrometer operating in a static field of 11.7 T. The samples, activated under vacuum at 80 °C for 4 h, were filled into a 4 mm zirconia rotor and spun at 5 kHz. The recycle delay was 30 s, in accordance with the phosphorus spin lattice relaxation times, and the number of accumulations was 64. The chemical shift was referenced with respect to external 85% H_3PO_4.

UV–vis spectrsoscopy. UV–vis adsorption spectra of HPA in solutions were acquired using a SPECOL 11 spectrophotometer from Carl Zeiss, Jena. UV–vis diffuse reflectance spectra of solid samples were measured on a SPECORD M-40 at 12,000–30,000 cm^{-1}, using MgO background.

2.3. Adsorption and thermal decomposition studies

N_2 adsorption isotherms were measured on an ASAP 2010 Micromeritics. Samples were activated under vacuum at 200 °C for 24 h. Specific surface area, pore size distribution and pore volume were determined using the Micromeritics software.

Table 1
Concentration of grafted function on the different supports.

Onium silica support		Concentration of grafted function (μmol g^{-1})		
		Cations		Chloropropyl groups
Py-1	*N*-pyridiniopropylsilica	Pyridinium	253	112
Py-2	*N*-pyridiniopropylsilica	Pyridinium	480	450
MeIm	(γ-(N,N′-methylimidazolio)propylsilica	Methylimidazolium	182	236
BuIm	(γ-(N,N′-butylimidazolio)propylsilica	Butylimidazolium	156	345

Thermal programmed decomposition (TPD) was performed on a TPD/R/O 1100 Thermoquest instrument equipped with TCD. The sample (0.05–0.1 g) was placed in a quartz tube, heated at 5 °C/min in He flow at 20 ml/min.

Thermal programmed decomposition followed by mass spectrometry (TPD MS, on Selmi MX 7304 A) was performed by heating the sample, pre-activated *in situ* at 25 °C and 10^{-3} Pa for 20 min, in vacuum ($p < 10^{-3}$ Pa) with heating rate 0.150 °C/s rate.

3. Results and discussion

3.1. Peculiarities of anion exchange on oniumsilica

For silica-based anion-exchanging materials, the anion-to-cation selectivities and binding constants depend on the lipophilicity of the exchanging anion [20,21]. Hence, the exchange of chloride by HPA anion is favoured due to the greater affinity of the hydrophobic cation for the hydrophobic HPA anion than for a hydrophilic Cl^-. As reported earlier, anion-exchange reactions on silica-immobilized onium salts proceed more easily when acids are used rather than their salts [20,21]. Indeed, the salts are less readily adsorbed by the functionalized silica support than the corresponding acids: greater charge separation requires more polar interaction than the support can provide [20,21]. For this reason, to achieve high exchange yields we used solutions of heteropolyacids and not their salts (in EtOH or MeCN). It was found important to use non-dried solvents to afford good solvation of the onium chloride silica, HPA dissolution and HCl removal. However, purely aqueous solutions were also not appropriate, because of the weak solvation of the resulting hydrophobic salts and because they favour HPA decomposition.

Ion exchange on the surface of onium supports, with the use of the acids $H_3PMo_{12}O_{40}$ and $H_3PW_{12}O_{40}$, can give salts of the types SiO_2–Q·H2A, SiO_2–Q_2·HA and SiO_2–Q_3·A (or, of SiO_2–Q_X·H_{3-X}A type, where x is a fraction, if calculated per material bulk).

Formation of SiO_2–Q·H_2A is assumed to proceed readily due to the good adsorption affinity of the hydrophilic surface for the hydrophilic HPA. Ionic bonds formed in neutral salts are stronger than in the corresponding acid salts [20,21], making the initial acid salt SiO_2–Q·H_2A thermodynamically less favoured; it should, therefore, get converted into SiO_2–Q_2·HA and SiO_2–Q_3·A. However, for such a transformation the distances between the grafted ligands have to satisfy the steric requirements. Retention of the acid salts is therefore also possible.

3.2. HPA concentration and composition of salt

The oniumsilica supports Py-1, Py-2 (*N*-pyridiniopropylsilica), MeIm (γ-(N,N′-methylimidazolio)propylsilica and BuIm γ-(N,N′-butylimidazolio)propylsilica were described earlier [19]. Table 1 reports the concentrations of grafted functions on these supports.

HPA concentrations achieved for each onium silica after exchange with HPA are given in Table 2 (before and after the hot wash) and 3 (after the hot wash only). Based on these concentrations, and the concentrations of onium functions, the surface salts

Table 2
Concentration of HPA (C_{HPA} per gram of starting silica) in the Py-1 and Py-2 sets for as-prepared catalysts (1) and after 12 h wash with hot MeCN (2). *X* = cation-to-anion ratio.

Catalyst	C_{HPA} (μmol g^{-1}, ±5)		*X* = Q-to-A ratio	
	1	2	1	2
Py-1-SiW	99	99	2.55	2.55
Py-1-PW	85	75	3.00	3.40
Py-1-PMo	103	82	2.45	3.10
Py-2-SiW	151	151	2.95	2.95
Py-2-PW	107	102	4.20	4.40
Py-2-PMo	140	105	3.25	4.35

of triprotic HPA can be described by the formula SiO_2–Q_X·H_{3-X}A, where Q stands for onium cation, A for HPA anion, and *X* is the Q-to-A ratio (Fig. 1). *X* = 3 corresponds to 100% exchange; *X* < 3 corresponds to the formation of an acid salt and *X* > 3 indicates that some of the surface groups do not participate in the reaction. Likewise, the surface salts of tetraprotic HPAs can be described by the formula SiO_2–Q_X·H_{4-X}A.

The values of *X* > 3 for Py-2-PW (4.4) and Py-2-PMo (4.35) samples, and at a lower extent for Py-1-PW (3.4), indicate that some of the surface groups do not participate in the ion-exchange reaction. Generally, a much higher exchange yield was achieved for Py-1 with monomeric silane coverage: (*X* = 3.4 for Py-1-PW and *X* = 3.1 for Py-1-PMo). Apparently, the support Py-2 with polysiloxane coverage has a greater proportion of inaccessible pyridinium groups than Py-1.

The greatest yield was obtained with $H_4SiW_{12}O_{40}$ acid (Table 2, lines 1 and 4). For this acid, the cation-to-acid ratio indicates the formation of the acid salts $(Py\text{-}1)_{2.55}H_{1.45}[SiW_{12}O_{40}]$ and $(Py\text{-}2)_{2.95}H_{1.05}[SiW_{12}O_{40}]$ (Fig. 1). This observation is consistent with the results obtained for NO_3^- anion exchange with HPA on double-pillared hydroxides $Zn_2Al(OH)_6NO_3{\cdot}H_2O$ [22]. The authors show that the exchange proceeds more easily for the highly charged (6^-, 7^-) anions, such as $[PW_9V_3O_{40}]^{6-}$ and $[SiW_9V_3O_{40}]^{7-}$, while no exchange was observed with 3^- or 4^- charged anions.

Part of the HPA contained in the materials, apparently, which is physically adsorbed, leaches into hot MeCN (Table 2), but the

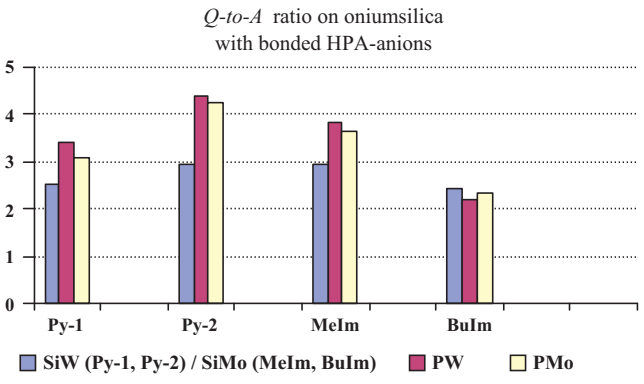

Fig. 1. Exchange yields of heteropolyacids with oniumsilica: comparison of four sets.

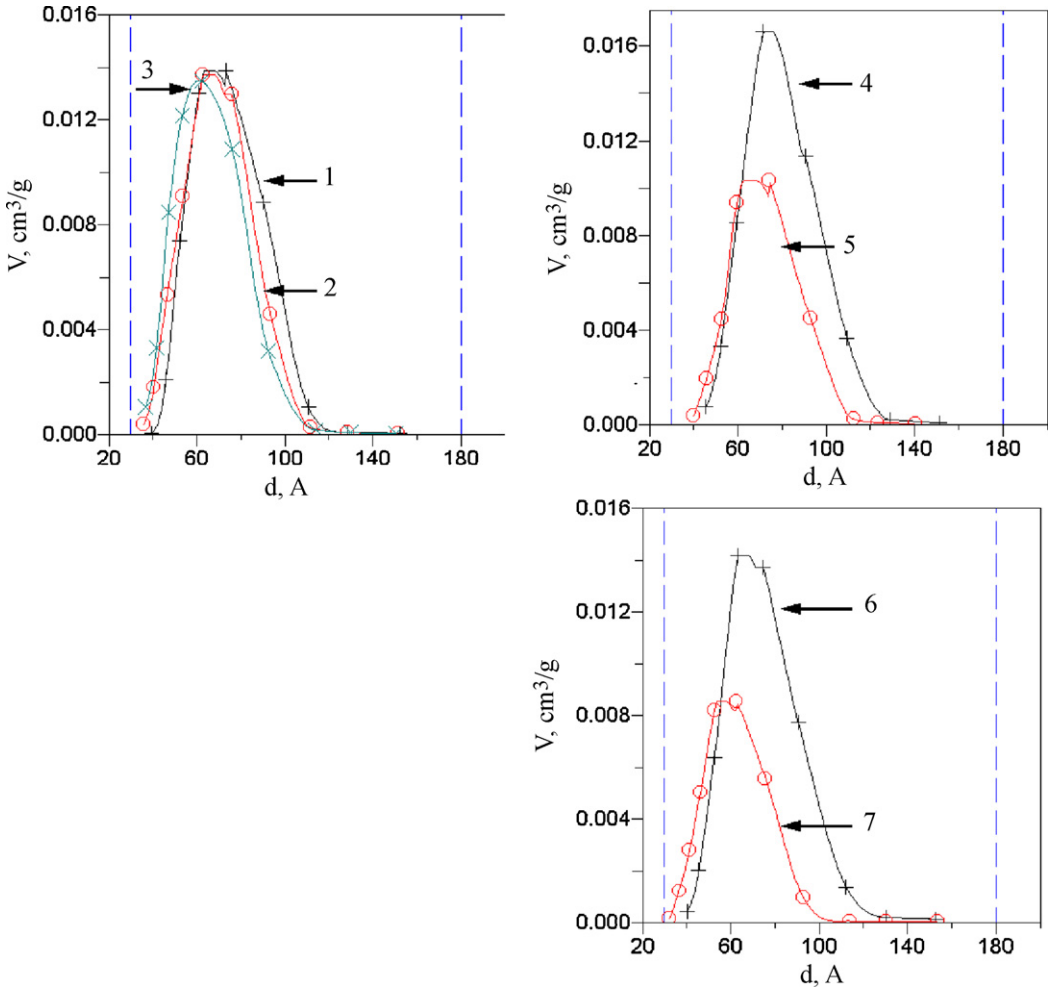

Fig. 2. Pore size distribution curves from N_2 desorption branch for MeIm/BuIm (1); MeIm-PW (2); BuIm-PW (3); Py-2 (4); Py-2-PW (5); Py-1 (6); Py-1-PW (7).

residue is resistant even to hot-water wash. The salts formed with $H_4SiW_{12}O_{40}$ are exceptionally stable to leaching, perhaps due to the stronger electrostatic interaction of a 4^- charged anion with the surface, and the greater hydrolytic stability of this anion itself.

With two sets of imidazolium-silicas greater exchange yields were achieved for all HPAs used (Table 3). We attribute this behaviour to the better accessibility of bound groups in these silicas due to the lower density (compare above-given concentrations of functional groups in pyridinium and imidazolium silica). The greater degree of chloride exchange and, consequently, the formation of the acid salt of formula $(BuIm)_2H_1[A]$ (triprotic acids) or $(BuIm)_2H_2[A]$ (tetraprotic acids) is favoured in the BuIm-HPA set, as compared to MeIm-HPA. Considering that both these supports were synthesized starting from one chloropropylsilica, the higher exchange yield of HPA with BuIm-silica should be related to the larger size and greater softness of the butylimidazolium cation.

Table 3
Concentration of HPAs (C_{HPA} per g of starting support) in MeIm and BuIm sets determined by X-ray fluorescence. Q-to-A is cation-to-anion ratio. C_{HPA} in brackets by P-elemental analysis.

Sample	C_{HPA}, $\mu mol\,g^{-1}$, ±5	Q-to-A ratio
MeIm-SiMo	62	2.95
MeIm-PW	47	3.85
MeIm-PMo	50 (64)	3.65 (3.00)
BuIm-SiMo	63	2.45
BuIm-PW	70	2.20
BuIm-PMo	66 (53)	2.35 (2.90)

This cation has a more pronounced phase-transfer action, as it has a hydrophobic butyl function directed into the silica pore.

Summarizing the preparation results, the Cl^- to HPA exchange was successful, while varying cation-to-acid ratios were attained using different cations and heteropolyacids (Fig. 1). The highest exchange ratio was obtained by: (a) using the supports with the lower density of organic functions (Py-1) as well as a more pronounced hydrophobicity of the latter (BuIm); (b) using the tetraprotic acids $H_4SiW_{12}O_{40}$ or H_4SiMoO_{40}. We presume this is firstly due to the greater charge (4+) and softness of these anions and, secondly, to stronger electrostatic interaction with the surface. Desirable acid salts with composition $Q_XH_{(4\text{ or }3)-X}[A]$ are most probably formed within Py-1-SiW, Py-2-SiW, MeIm-SiMo, and all BuIm-HPA solids.

3.3. Textural characteristics from XRD and N_2 adsorption

It should be noted that XRD does not show the presence of crystalline HPA in any sample prepared. However, the same silica supports, non-functionalized, that contain similar amounts of HPA loaded via impregnation (up to *ca.* 25 wt.%), reveal significant crystallinity. This result points out the excellent distribution of HPA on the surface of our samples.

N_2 adsorption (Table 4 and Figs. 2 and 3) was carried out only on all PW-immobilized samples, assuming that the other samples, prepared with the others HPAs in each set, have analogous characteristics.

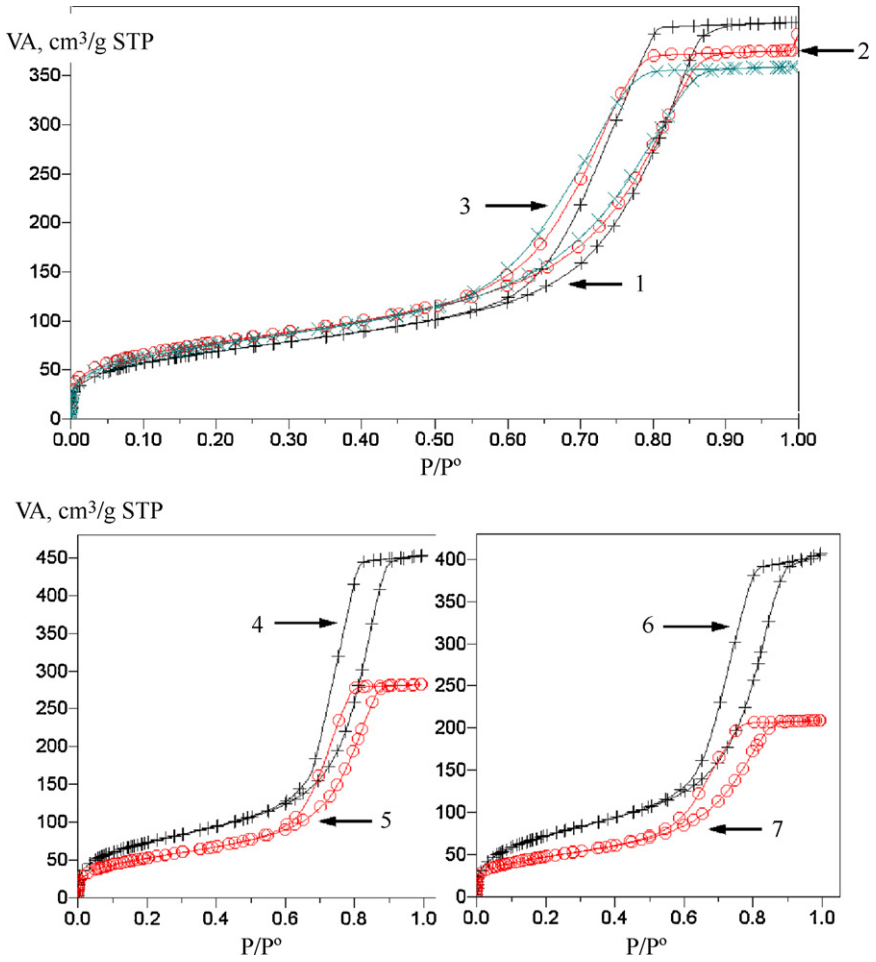

Fig. 3. N_2 adsorption/desorption isotherms for MeIm/BuIm (1); MeIm-PW (2); BuIm-PW (3); Py-2 (4); Py-2-PW (5); Py-1 (6); Py-1-PW (7).

Isotherms of N_2 adsorption on the starting onium silica supports and functionalized solids are of the classical IV-type shape, typical of amorphous siliceous solids, with a II-type hysteresis loop (Figs. 2 and 3).

All grafted silica supports used (MeIm, BuIm, Py-1 and Py-2) have specific surface area and corresponding pore volume slightly smaller than the starting silica. But the mean pore diameters are roughly the same (Table 4).

Comparison of the BET surface areas before and after immobilization of HPA on pyridinium-silicas and imidazolium-silicas indicates two different types of changes, brought about by immobilization.

The S_{BET} values (specific surface area per g of catalyst) of pyridinium-silica-based catalysts, Py-1-PW and Py-2-PW, fall by around 30%, compared to that of the starting pyridinium-silicas, Py-1 and Py-2. One has to consider very high wt.% concentrations of grafted PW acid. The pore diameters and pore volumes decrease even more significantly: pore volumes by *ca.* 40–50%, mean pore diameter by 6 and 12 Å, respectively. However if one presents the results normalized to 100 wt.% of the intial support Py-1 and Py-2, the surface values, denoted S'_{BET}, and the corresponding pore volumes, are closer to those of initial supports Py-1 and Py-2 (Table 4).

Table 4
Characteristics of onium salts with $H_3PW_{12}O_{40}$: S_{BET} (specific surface area per g of catalyst), V (corresponding pore volume), d (mean pore diameter). In brackets are the respective values of S'_{BET} (specific surface area per g of starting onium silica support) and corresponding V' (pore volumes per gram of starting support).

Sample	S_{BET}, $m^2\ g^{-1}$ (S'_{BET}, $m^2\ g^{-1}$)	d, Å	V, $cm^3\ g^{-1}$ (V', $cm^3\ g^{-1}$)
Starting SiO_2	297.3	72.0	0.77
MeIm, BuIm	254.5	71.7	0.63
MeIm-PW	285.3 (325.7)	67.2	0.58 (0.66)
BuIm-PW	278.4 (336.8)	63.6	0.56 (0.68)
Py-1	272.4	77.0	0.69
Py-1-PW	193.1 (235.6)	69.9	0.44 (0.54)
Py-2	275.6	72.1	0.61
Py-2-PW	172.0 (223.4)	60.3	0.32 (0.42)

For imidazolium-silica-based catalysts, MeIm-PW and BuIm-PW, we observe a decrease in the mean pore diameter and volume, but with a significant increase in S_{BET}. This "atypical" phenomenon is even more noticeable when the surface is normalized per gram of starting support (S'_{BET} = 325.7 and 336.8 for MeIm-PW and BuIm-PW, respectively). Moreover, the normalized per gram of pore volumes of these samples are very close to the initial values.

Such an "atypical" increase in the specific surface area can be explained in the framework of the following model: anions are distributed on the surface in a uncompleted monolayer and do not touch each other. In this case the specific surface area per gram of catalyst is equal to the sum of the surface area of the starting support S_{BET} (multiplied by its weight impact) and of the area, S', added by each sphere of HPA anions {calculated as the surface area of a sphere ($4\pi R^2 \equiv 3.08\ nm^2$ per anion $\equiv 620\ m^2\ g^{-1}$ of HPA); minus the surface area of support covered by HPA anions, (taken as $1.44\ nm^2$ per anion $\equiv 290\ m^2\ g^{-1}$ of HPA)}, multiplied by its weight impact. In this case, the surface areas of the catalysts are, in $m^2\ g^{-1}$:

$$S(\text{MeIm-PW}) = S(\text{MeIm}) \times 87.6\% + S'(\text{HPA}) \times 12.4\%$$

$$= 223 + 41 = 264(\text{experimental value } S_{BET}285)$$

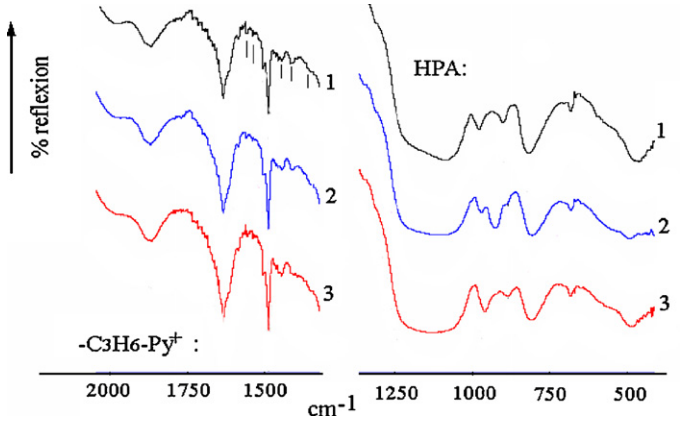

Fig. 4. DRIFT spectra (ambient conditions) of the Py-2-HPA catalyst set: Py-2-PW (1); Py-2-SiW (2); Py-2-PMo (3).

$$S(\text{BuIm-PW}) = S(\text{BuIm}) \times 82.6\% + S'(\text{HPA}) \times 17.3\%$$
$$= 210 + 57 = 267(\text{experimental value } S_{\text{BET}}278)$$

This calculation shows that this HPA distribution model describes the situation quite adequately; very good distributions of HPA anions are attained for the two samples, MeIm-PW and BuIm-PW.

For the pyridinium-silicas (in particular, Py-2) with much higher concentrations of HPAs (where the anion concentration approaches the theoretical monolayer coverage and their clustering can begin), the calculated values of the surface areas sgnificantly exceed the experimental ones.

$$S(\text{Py-1-PW}) = S(\text{Py-1}) \times 82\% + S'(\text{HPA}) \times 18\%$$
$$= 223 + 60 = 283(\text{experimental value } S_{\text{BET}}193)$$

$$S(\text{Py-2-PW}) = S(\text{Py-2}) \times 77\% + S'(\text{HPA}) \times 23\%$$
$$= 210 + 76 = 286(\text{experimental value } S_{\text{BET}}172)$$

This means that for pyridinium silicas, the distribution of HPAs may be worse than in the case of alkylimidazolium salts. Since the mean pore diameter for both Py-based samples also falls considerably, the decreased surface areas can be explained and fitted based on the model of cylindrical pores with walls fully covered with HPA and, therefore, with a diameter reduced by two diameters of HPA anion.

The results obtained from nitrogen adsorption evidence that: (1) the catalysts with grafted onium-HPA salts preserve sufficiently high surface areas and pore volumes; (2) HPA is well dispersed over the catalyst surface, forming a monoanionic layer, at least for imidazolium silicas; (3) the pores and a major part of the catalyst surface remain accesible.

3.4. Chemical characterization of the oniumsilica-HPA salts

3.4.1. DRIFT at ambient temperature

All catalysts sets were studied, however, as an example, DRIFT spectra of one catalysts set, Py-2-HPA, are shown in Fig. 4. Absorptions due to the *N*-pyridiniopropyl cation at 1640, 1585, 1502, 1588, 1446, 1417, 1360 and 1314 cm^{-1} are unaffected compared to the precursor Py-2. Based on the FTIR data reported for various heteropolyoxometalates and precipitated pyridinium salts [23–27], the absorptions due to the ν(M=O) and ν(M–O–M) in the HPA structure indicate that the immobilized anions conserve an intact Keggin structure: $[PW_{12}O_{40}]^{3-}$: 980, 900, 815 cm^{-1}; $[SiW_{12}O_{40}]^{3-}$: 970, 924, 885, 805 cm^{-1}; $[PMo_{12}O_{40}]^{3-}$: 958, 885, 810 cm^{-1}.

DRIFT spectra of the other catalysts, similar to the spectra presented, confirm the structure of the grafted onium salt as well as the intact Keggin structure of the immobilized heteropolyoxometalates.

3.4.2. ^{31}P SPE-MAS NMR

The ^{31}P SPE-MAS NMR spectra of the prepared samples of both the $[PW_{12}O_{40}]$ and $[PMo_{12}O_{40}]$ anions indicate that the immobilized anions maintain the Keggin structure intact [24,27–29]. The spectra obtained for some of the samples are given in Fig. 5. There is no significant difference in the chemical shifts of free and immobilized anions.

In the case of $[PW_{12}O_{40}]$-based catalysts only the peak at −15 ppm, characteristic of the corresponding Keggin structure, was detected. In the case of samples with immobilized $H_3PMo_{12}O_{40}$, in addition to the peak of the intact Keggin anion located at *ca.* −3.2 ppm [23], the spectrum shows another peak, of very weak intensity at *ca.* −1.5 ppm. This peak was assigned to phosphate groups resulting from decomposition of $H_3PMo_{12}O_{40}$ during its immobilization [25,26]. According to intensities ratio, there is decomposition of up to 5% of immobilized anions.

Similar to the spectra recorded for silica-adsorbed HPA [28], the peaks corresponding to Keggin anions are very narrow and have symmetrical shape. This indicates that the HPA are not markedly distorted by bonding to the surface via onium salts.

3.4.3. Red-Ox state of HPA anions: UV–vis diffuse reflectance spectra

UV–vis spectra of HPA contain ligand-metal charge transfer (LMCT) transition bands around 200–400 nm. It has been shown that the spectra depend strongly on the dispersion of HPA on the support: for silica-supported $H_4SiMo_{12}O_{40}$ the lowest energy LMCT band blue-shifts and narrows with increasing HPA dispersion [30]. Moreover, the spectra are influenced by the reduction state of the immobilized HPAs, as well as by their structure: the transformation of Keggin anions into lacunary anions is reflected by the new bands, *e.g.* 215 and 295 nm of $PMo_{11}O_{39}^{7-}$ [23].

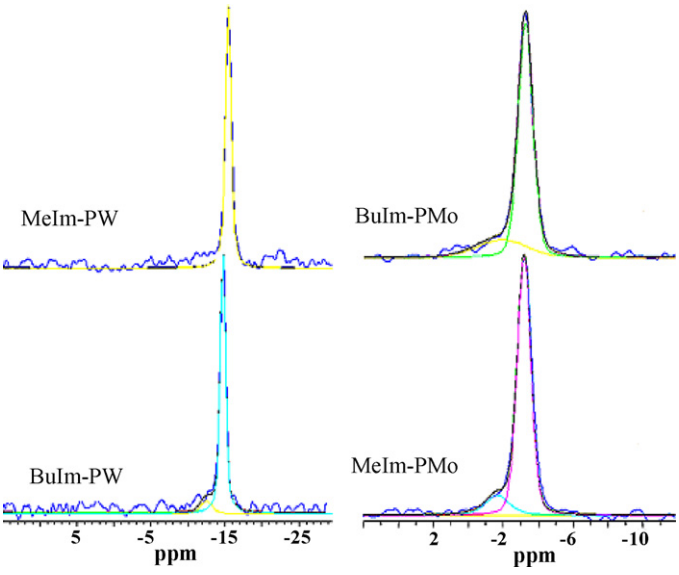

Fig. 5. ^{31}P SPE-MAS NMR spectra of $H_3PW_{12}O_{40}$ and $H_3PMo_{12}O_{40}$ immobilized on MeIm, BuIm silicas: experimental spectra (bluemarine), sum of the whole fitted lines (black), individual fitted lines (other colours: blue, yellow, red, green). (For interpretation of the references to colour in this figure legend, the reader is referred to the web version of this article.)

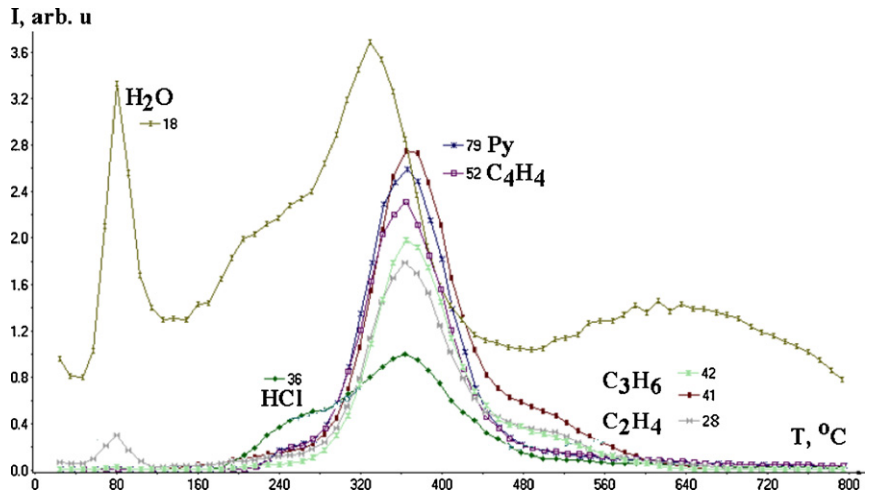

Fig. 6. TPD MS decomposition of Py-1-PW.

The absorption maxima in the spectra (not shown here) of our fresh catalysts correlate with those of precursor HPA (recorded as a *ca.* 20 wt.% mechanical mixture with SiO_2): 345 nm ($H_3PW_{12}O_{40}$), 357 nm (Py-2-PW); 345 nm ($H_4SiW_{12}O_{40}$ and Py-1-SiW, Py-2-SiW); 357 nm and a shoulder at *ca.* 435 nm ($H_3PMo_{12}O_{40}$ and Py-2-PMo). A blue shift of the lowest energy LMCT band, compared to that in the spectrum of a starting acid, confirms that the acids are well dispersed. The spectra of fresh samples do not display any noticeable features around 600–800 nm that might be attributed to reduced heteropolyanions (so-called heteropolyblues).

3.4.4. Partial conclusion

In conclusion to the characterization section, it can be stated that anion exchange of HPAs with silica-grafted onium salts results in solids with intact structure of onium cations and relatively intact structure of HPA anions. Immobilization of the molybdenum-based acid, $H_3PMo_{12}O_{40}$, however, is accompanied by its decomposition to some degree.

3.5. Thermal stability of onium-HPA salts

The thermal stability of the grafted onium-HPA salts was studied by means of three parallel techniques. DRIFT Spectroscopy with *in situ* thermal treatment of the samples under N_2 flow allowed examination of the species produced on the surface of the functionalized silicas during their decomposition. TPD followed by MS was applied to monitor the volatile products evolved during the decomposition of the onium-HPA salt (studied for one representative sample, Py-1-PW). The products of the thermal decomposition of all other catalysts were examined using thermal programmed decomposition in He flow followed by analysis of the desorbed gases by conductivity measurements with the use of TPD/R/O equipement. The decomposition peaks were attributed using the results of TPD–MS and DRIFT.

3.5.1. TPD–MS of Py-1-PW

Thermal decomposition of the catalyst Py-1-PW proceeds in several stages. Water is evolved in four stages (Fig. 6): – desorption of adsorbed water at *ca.* 90 °C; – both the desorption of the water hydrogen-bonded to HPA anions and the condensation of vicinal silanols at *ca.* 160–250 °C; – loss of constitutional water from HPA and, subsequently, its decomposition at *ca.* 340 °C; – condensation of the residual silanols of the silica at 560–700 C.

Decomposition of the organic layer proceeds in three stages: (a) at 240 °C only HCl is evolved, presumably due to the decomposition of unreacted pyridinium chloride, as in the TPD MS of the initial Py-1. However, no peak due to pyridine appears at this stage, which is due to the strong adsorption of pyridine on acid sites of Py-1-PW. (b) The main decomposition proceeds at *ca.* 300–460 °C (max. at *ca.* 380 °C), with evolution of pyridine (*m*/*z* 79), C_4H_4 (*m*/*z* 52), HCN (*m*/*z* 27), HCl (*m*/*z* 35, 36), C_3H_6 (*m*/*z* 42, 41, 43) as well as other fragments of the propyl chain (CH_4, C_2H_4, C_2H_2) (Fig. 6). (c) At 480–560 °C, C_3H_6 and C_2H_4 are produced, due to the decomposition of the residual propene groups formed during stage b, similarly to what is observed in the TPD MS of the initial Py-1 [19].

3.5.2. Thermal stability of all pyridinium-HPA salts

3.5.2.1. DRIFT-TPD. Set Py-2-HPA. The results obtained are presented in Fig. 7 and Table 5. The bands were assigned on the basis on [31,32]. Several processes by which solids thermally decompose were found to occur, consistent with the results of TPD MS. In addition, an important process, namely secondary pyridine adsorption during decomposition, was detected.

The spectrum of Py-2-PMo (25–200 °C) displays characteristic absorbances due to aromatic and propyl chain C–H stretching, pyridine ring-stretch vibrations (Table 5) and M=O/M–O–M vibrations in the Keggin structure of the immobilized HPA (959 and 884 cm^{-1}). Physically adsorbed water and hydrogen-bonded water are mostly removed from the surface at 100 °C, as shown by the disappearance of the bands at 3337–3400 cm^{-1} and 1620 cm^{-1}. The C–H stretches of the propyl chain and, to a certain extent, of the pyridinium cation remain unchanged up to 200 °C. The spectrum starts to change significantly at 250 °C, where it displays new NH aromatic stretches (3206 cm^{-1}), C–H aromatic stretches (3126, 3090, 3056 cm^{-1}), ring C=C and C=N stretches (1525, 1603 cm^{-1}) and pyridine fingerprint vibrations (758 cm^{-1}) (Table 5). These are the bands that can most probably be ascribed to the protonated pyridine generated on the surface (the mechanism will be discussed below). At 250 °C new C–H stretches are displayed (3005–2980 cm^{-1}), indicating formation of an alkene group. As shown by the spectra in the region below 1000 cm^{-1}, at 250 °C the initial Keggin structure begins to break down: the band at 959 cm^{-1} is broadened and transformed into 954 cm^{-1}; the band at 884 cm^{-1} disappears, and instead a broad shoulder at 920 cm^{-1} is observed. Decomposition of the residue of pyridinium cation and propyl chloride together with the desorption of pyridine proceeds only at 350 °C in air. At the same time very strong bands at 3747 cm^{-1} and 985 cm^{-1} (≡SiO–H and ≡Si–OH stretch) appear due to the thermolysis of Si–C and Si–OH formation. In addition, new bands are observed in the lattice vibration region at 1190, 1160, 1054 and 1033 cm^{-1}.

Table 5
IR spectral data for Py-2-HPA at different temperatures. Bands appearing during decomposition are in italic. (Str, stretch; KS, Keggin structure).

Sample	*T*, °C	Pyridinium/pyridine		C–H, aliphatic chain	P–O, M=O, M–O–M KS and silica	Other bands due to silica
		C–H/N–H str	Ring, C=C, C=N, fingerprints			
Py-2-PW	100	3133, 3090, 3067 (C–H of Py^+)	1632, 1488, 680 (Py^+)	2956, 2940, 2896, 1445, 1409	1104 (Si–O and P–O), 979 (M=O) 899 (M–O–M), 815 (Si–O–Si, M=O)	3640 (vicinal SiO–H), 3337 (O–H str, H-bonded water)
	100–200 250–350	Similar *3204 (PyH^+, N–H str); 3050, 3141 (PyH^+, C–H str)*; 3123, 3089 (-Py^+ C–H)	Similar 1632, 1480, 680 (Py^+) *1602, 1527, 752 (PyH^+)*	Similar 2941, 2902, 2863, 2792, 2650; 3012, 2984 (sp^2-C–H)	Similar 1102 (Si–O and P–O), 1056, 985 (Si–OH); *960, 892* (M–O–M and M=O in decomposed KS), 812 (Si–O–Si, M=O)	Fading of 3337 *3737 (isolated SiO–H)*, 3640 (vicinal SiO–H str)
	350 in air	All disappear	All disappear	All disappear	1160, 1102 (Si–O), 1056, 985 (Si–OH), 960, 892 (M=O in decomposed KS), 812 (Si–O–Si, M=O)	Growth 3737 (isolated SiO–H), 3640 (vicinal SiO–H str)
Py-2-SiW	100	3126, 3084, 3064 (C–H of Py^+)	1631, 1485, 682, 1445 (–Py^+)	2960, 2938, 2895, 1409	1160, 1053 (Si–O and P–O), 971, 922, 885, 804 (M=O, M–O–M of KS, Si–O–Si)	3666 (vicinal SiO–H), 3213 (O–H str, H-bonded water
	200–250 350	Similar *3204 (PyH^+, N–H str); 3051, 3142 (PyH^+, C–H str)*; 3125, 3087 (C–H of Py^+)	Similar *1602, 1528, 760 (PyH^+)*; 1632, 1483, 1441, 1391, 682+(–Py^+)	Similar 2940, 2902, 2865, 2795, *2651; 3007, 2982* (sp^2-C–H)	Similar *1238, 1189, 1153, 1055 and 1031 (Si–O and P–O)*, 922→997 (partially Si–OH), 971 and 885 (M=O, M–O–M of KS are fading), 804 (Si–O–Si and M=O)	Fading of 3217 Growth *3737* (isolated SiO–H), 3640 (vicinal SiO–H str)
	350 in air	All disappear	All disappear	All disappear	Restoring of 1055, 971, 927, 885, 804 (KS)	3737 (isolated SiO–H str), 3640 (vicinal SiO–H str), 1620-H-bonded water
Py-2-PMo	25	3132, 3092, 3067, 3033 (C–H of Py^+)	1649, 1634, 1622, 1488, 682 (Py^+)	2980, 2939, 2900, 1457	1160, 1060 (Si–O, P–O); 959, 884, 804 (Mo=O, Mo–O–Mo KS, Si–O–Si)	3300-3400 (O–H str, H-bonded water)
	100 200–350	Similar *3206 (PyH^+, N–H str), 3056 (PyH^+, C–H str)*; 3126, 3090 (C–H of Py^+)	Similar 1650, 1631, 1558, 682, 1482 (Py^+); *1603, 1525, 1508, 758* (PyH^+)	Similar *3005-2980 (sp^2-C–H)*; 2978, 2941, 2892, 1457	Similar 1190, 1160, 1060 (Si–O, P–O)→ *1054* and *1033*; 959→ *954*, 884→ *920*, 808 (Mo–O–Mo, Mo=O in decomposed KS, Si–O–Si)	Fading 3400 3747 (isolated SiO–H; Si–C thermolysis), 3660 (vicinal SiO–H str), 1620-H-bonded water

Decomposition of the organic layer of Py-2-PW occurs at 250–300 °C, as with Py-2-PMo (Table 5). At this stage, the Keggin structure is still intact. Its decomposition, beginning at 350 °C, is detected by the broadening of the initially observed bands at 979 and 899 cm^{-1} and the appearance of bands at 960 and 892 cm^{-1}. Decomposition of the organic layer in Py-2-SiW proceeds similarly. The immobilized acid, $H_4SiW_{12}O_{40}$, turns out to be highly thermally stable. Disturbance of the bands due to its Keggin structure begins at 350 °C, but exposure of the sample to wet air almost restores the *status quo* (Fig. 7).

Decomposition of the Py-1-HPA set samples proceeds in the same way as for Py-2-HPA (the DRIFT-TPD profiles for Py-1-HPA group of catalyst are not shown). Decomposition of the anion in Py-1-HPA begins at a lower temperatures than for Py-2-HPA (by *ca.* 50 °C), probably due to the smaller concentrations of immobilized HPAs. Like Py-2-HPA, the thermal stability of the Keggin structure of immobilized HPA increases in the following order: $H_3PMo_{12}O_{40}$ (disorder of the Keggin structure is observed already at 200 °C), $H_3PW_{12}O_{40}$ (decomposition begins at 300 °C), $H_4SiW_{12}O_{40}$ (disorder of the Keggin structure is observed at 250–300 °C, but in this case decomposition is reversible at this stage and after exposure to air the Keggin structure is partially reconstructed, due to the contact with moisture present in air). The silica in Py-1 contains smaller concentrations of grafted propylpyridinium and propyl chloride than that of Py-2 and, consequently, higher concentrations of the residual silanols. Decomposition of propyl chloride and propene–silica proceeds only upon exposure to air at 350 °C (in N_2 it is stable at $T > 350$ °C).

3.5.2.2. Monitoring of TPD of catalysts Py-1-HPA and Py-2-HPA with TCD measurements (Fig. 8). Our results show that the decomposition of HPA salts immobilized on pyridinium-silica is accompanied by the appearance of several peaks, which are consistent with the results obtained from the DRIFT-TD study and can be interpreted on that basis. The first peak around 95–120 °C corresponds to the desorption of physically adsorbed water. The decomposition temperature of the grafted salt depends markedly on the HPA: the decomposition of Py-2-PMo and Py-1-PMo proceeds at 276 °C and 284 °C, accompanied by evolution of water from decomposed $H_3PMo_{12}O_{40}$. Peaks corresponding to the total destruction of the grafted layer, involving residues of propene-silica and propyl chloride-silica, are observed at 418 °C. In the case of the more thermally stable acids, $H_3PW_{12}O_{40}$ and $H_4SiW_{12}O_{40}$, decomposition begins around 340 °C; total destruction of grafted salt is observed at 393 °C (Py-1-PW), 399 °C (Py-2-PW), 405 °C (Py-2-SiW) and 416 °C (Py-1-SiW). The HPA anion, residues of pyridinium cation, and grafted propyl chloride decompose simultaneously at this temperature, probably accompanied by the evolution of pyridine, water, propene and HCl. Condensation of residual silanols proceeds at 580–650 °C and is accompanied by a relatively weak peak of water, as a result of the low concentration of residual silanols.

As a result, several processes occurring in the course of the thermal destruction of HPA-onium salts on silica are now outlined:

(1) Firstly, there is a partial decomposition of the residual pyridinium chloride at low temperatures giving rise to the

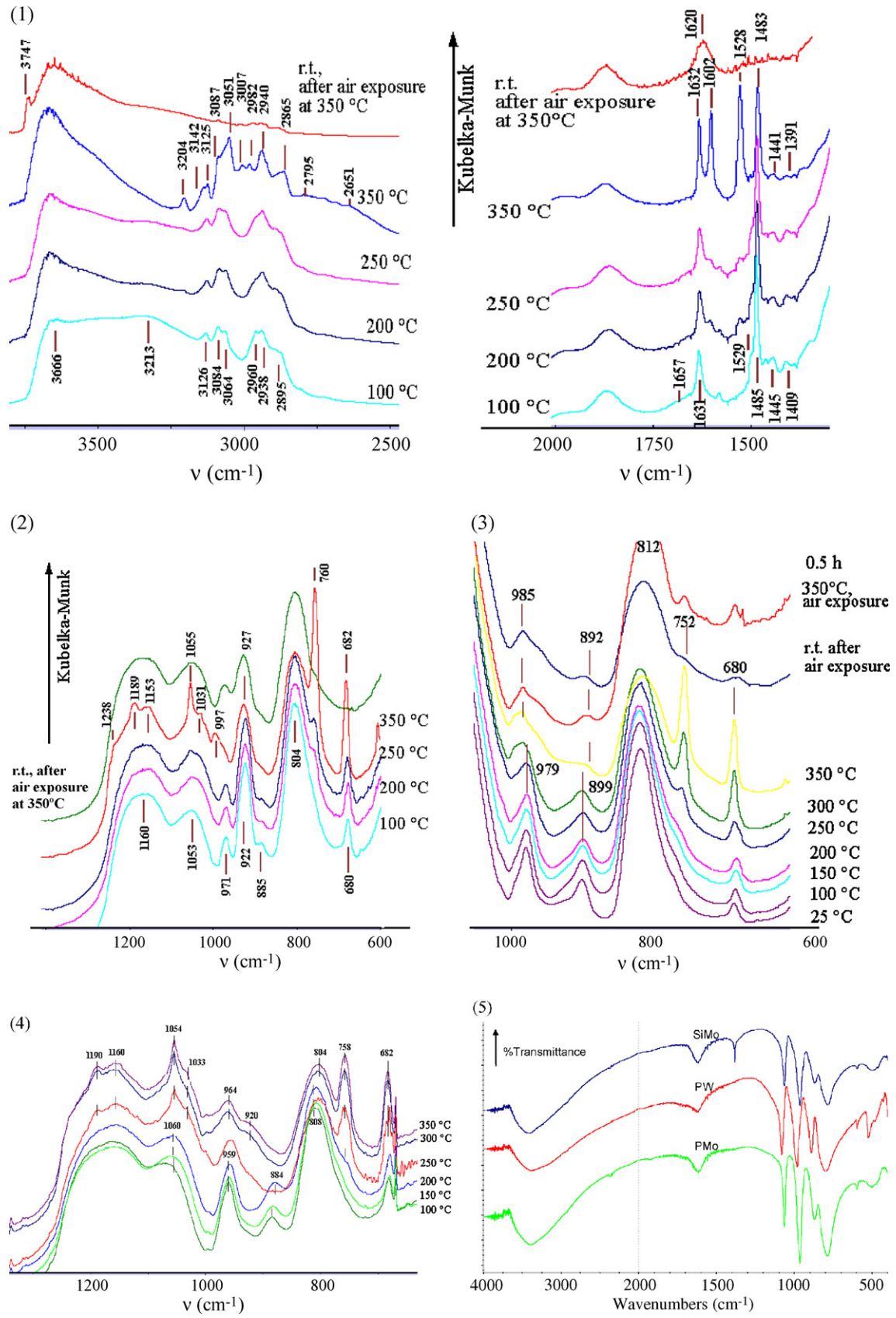

Fig. 7. (1) DRIFT monitoring of the decomposition of Py-2-SiW in N_2 flow (3750–1250 cm^{-1}). (2) DRIFT monitoring of the decomposition of Py-2-SiW in N_2 flow (1400–600 cm^{-1}). (3) DRIFT monitoring of the decomposition of Py-2-PW in N_2 flow (1100–600 cm^{-1}). (4) DRIFT monitoring of the decomposition of Py-2-PMo in N_2 flow (1400–600 cm^{-1}). (5) IR of the starting HPAs (pellets with KBr).

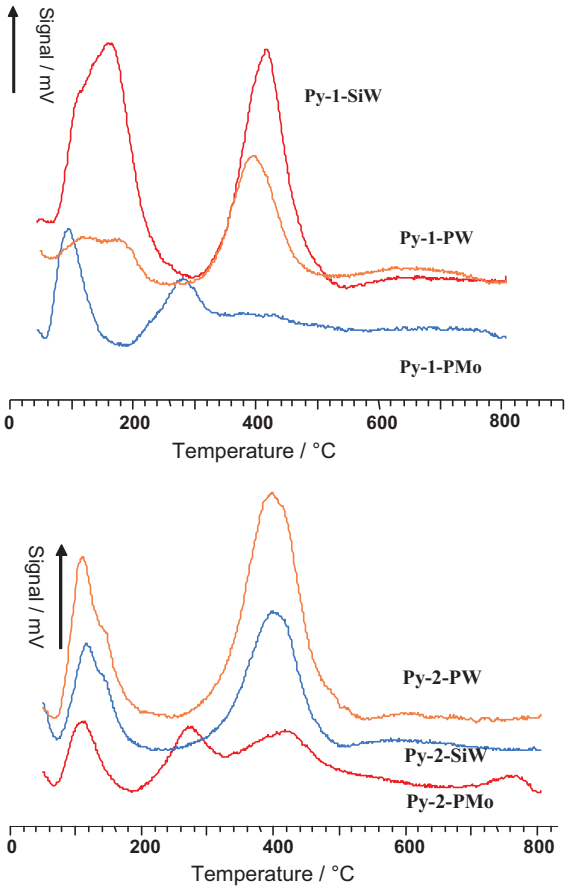

Fig. 8. TCD-monitoring of thermal decomposition of HPA salts immobilized on Py-1 and Py-2 silica.

formation of protonated pyridine (process 1). This process occurs at 250–300 °C, perhaps yielding also SiO_2–C_3H_5 (propene–silica). At this stage, the Keggin structure of the HPAs is still intact (with an exception of PMo). Pyridine remains adsorbed on the surface until the samples are exposed to air at 300–350 °C.

(2) A further process, 2, is the destruction of the Keggin structure of heteropolyanions. The temperature at which this process occurs depends strongly on the nature of the HPA. The thermal stability of the Keggin structure of the immobilized HPAs increases in the following order: $H_3PMo_{12}O_{40}$ (200–250 °C) < $H_3PW_{12}O_{40}$ (300–350 °C) < $H_4SiW_{12}O_{40}$. Although slight disorder of the Keggin structure of the latter HPA is observed already at 250 °C, its decomposition at this stage remains reversible: after sample exposure to air, the Keggin structure is reconstructed, as a results from the contact with moisture.

(3) The third process is the decomposition of the organic residue, SiO_2–C_3H_5 and SiO_2–C_3H_6Cl, which requires $T > 350$ °C in N_2, but proceeds easily upon exposure to air at 350 °C (at 300 °C it is quite stable).

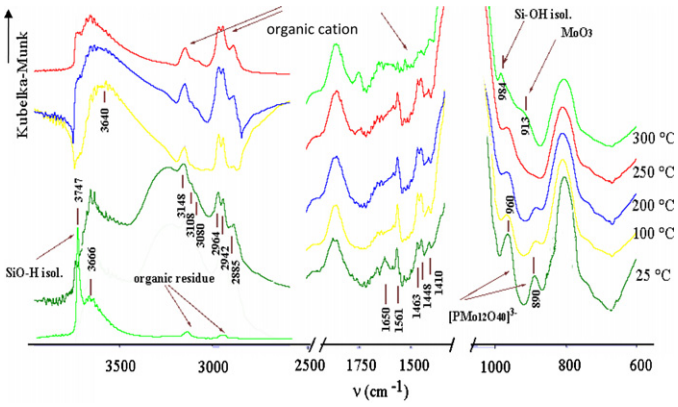

Fig. 9. DRIFT monitoring of the decomposition of BuIm-PMo in N_2 flow.

According to both TPD and DRIFT results, the pyridinium-HPA salts are characterized by high thermal stability. HPA salts, prepared from silica with monomeric (Py-1) and polymeric grafted layers (Py-2) display comparable thermal stability. The thermal stability of the Keggin structures of anion is slightly lower (PW and SiW) or lower than that of the parent acids. The grafted salts can be placed in an order of increasing stability, which coincides with the order of thermal stability of the precursor acids:

$$SiO_2\text{–}Py_3PMo_{12}O_{40}(\approx 280\,^\circ C) \ll SiO_2\text{–}Py3PW_{12}O_{40}(395\,^\circ C) \leq SiO_2\text{–}Py_4SiW_{12}O_{40}(410\,^\circ C).$$

3.5.3. *Stability of imidazolium-HPA salts*

DRIFT monitoring of the decomposition of HPA immobilized on imidazolium-silica was performed for the one sample: BuIm-PMo.

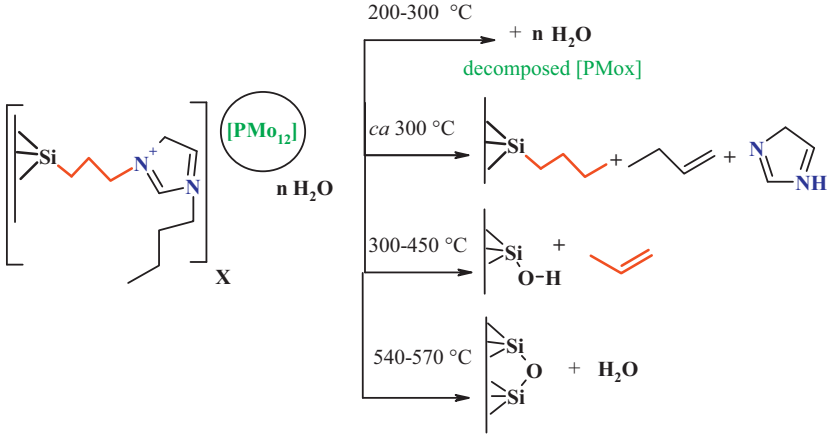

Scheme 1. Thermal decomposition of the salt of grafted N-propyl-N′-butylimidazolium cation with $H_3PMo_{12}O_{40}$ acid.

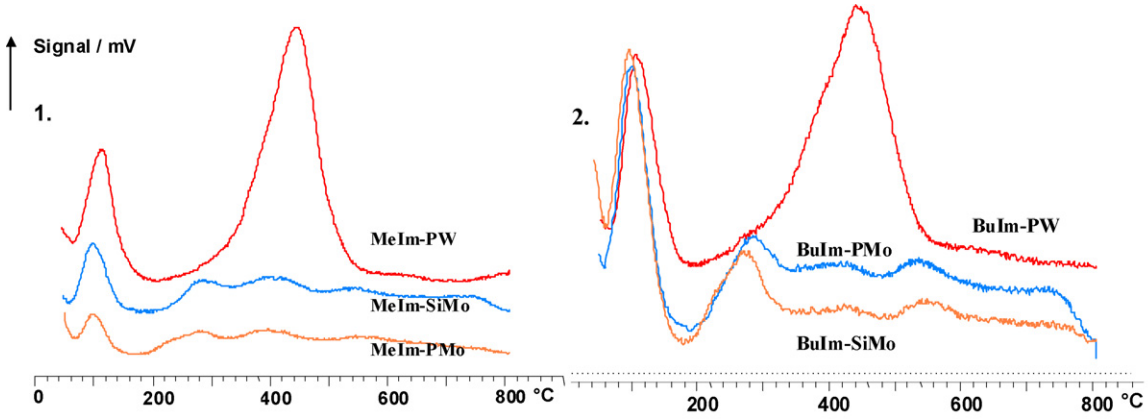

Fig. 10. TCD-monitoring of thermal decomposition of: (1) MeIm-HPA (red – MeIm-PW, blue – MeIm-SiMo, yellow – MeIm-PMo); and (2) BuIm-HPA: red – BuIm-PW, blue – BuIm-PMo, yellow – BuIm-SiMo. (For interpretation of the references to colour in this figure legend, the reader is referred to the web version of this article.)

The spectrum of the starting BuIm-PMo (Fig. 9) displays the following bands: 3640 cm^{-1} (SiO–H stretch, vicinal silanols), 3337 cm^{-1} (hydrogen-bonded water), 3147, 3109 and 3080 cm^{-1} (C–H stretch vibrations of imidazolium ring); 2964, 2942 and 2885 cm^{-1} (C–H stretches of propyl and butyl chains); 1651, 1561, 1448 cm^{-1} (ring stretches, imidazolium cation), 1463 and 1410 cm^{-1} (C–H deformations of propyl and butylimidazolium chains), 1104 cm^{-1} (Si–O and P–O stretching), 960, 890 and 807 cm^{-1} (Mo=O, Mo–O–Mo stretches in Keggin structure, band at 807 cm^{-1} overlaps with Si–O–Si), 740 and 700 cm^{-1} (fingerprints of imidazolium ring). Treatment of the sample at 250–300 °C results in the decomposition of the Keggin structure of $H_3PMo_{12}O_{40}$: initial bands at 960 and 890 cm^{-1} are broadened, finally yielding a new broad band at 913 cm^{-1}.

The organic layer is stable at 250–300 °C in N_2 but is decomposed at 300 °C in air, as can be deduced from the decrease in the intensities of bands corresponding to the organic function and simultaneous appearance of ≡SiO–H at 3743 and ≡Si–OH at 984 cm^{-1}. In contrast to pyridinium-HPA silica, no secondary adsorption of the products evolved during decomposition of the grafted layer occurs for immobilized $H_3PMo_{12}O_{40}$. Immobilized $H_3PMo_{12}O_{40}$, like Py-1(2)-PMo, starts to lose its Keggin structure at around 250 °C.

If decomposition is followed by measuring evolving gases, two to four peaks can be detected (Fig. 10): – at 97–110 °C desorption of physically adsorbed water; – at 270–290 °C water loss due to decomposition of the Keggin structure (SiMo and PMo anions), and transformation of methylimidazol and butylimidazol into propene fragments; – at around 300–450 °C a further decomposition of propyl-silica and propene–silica; – at 540–570 °C loss of water, formed due to silanol condensation. The thermal stability of immobilized PW salts is the greatest due to the stability of the precursor acid. These salts decompose in one stage at 300–500 °C.

These processes (example of BuIm-PMo and BuIm-PW) are tentatively described in Schemes 1 and 2.

3.6. Acidity overview

Acidity measurements on the described materials are presented in our previous paper [1], so here we only briefly recall the results. Considering the structure of the grafted salts, one expects there to be at the most two (= 3 – 1, for PW, PMo) or three (= 4 – 1, for SiW) Brønsted acid sites per Keggin unit as the result of the formation of the acid salt SiO_2–$Py^+(H_2A)^-$. As showed the results of elemental analysis (Tables 1 and 2), even smaller number of residual acid protons per Keggin Unit was obtained in surface-immoblized HPA salts (up to 0.5–1, see cation-to-anion ratio in Fig. 1).

The acid site number for all the oniumsilica-immobilized HPA was measured by ammonia adsorption at 25 °C. The number of NH_3 molecules adsorbed on the onium-HPA salts approaches 6 for most samples, which is extraordinarily high. It seems that the adsorption of ammonia under the experimental conditions proceeds by the reduction of the Keggin unit with ammonia, thus, the number of adsorbed ammonias does not directly reflect the number of Brønsted acid sites. What regards the acidity strength, we used another experiment, namely TEPO adsorption and measuring of its chemical shift (^{31}P). For pure HPA in bulk acidity is known to increase in the following order: $H_4SiMo_{12}O_{40} < H_3PMo_{12}O_{40} < H_4SiW_{12}O_{40} < H_3PW_{12}O_{40}$. We found that the acidity of the immobilized HPAs increases as follows: PMo ≈< PW < SiW (support Py-2), PMo < PW < SiW (support Py-1), PW ≈ <PMo ≪ SiMo (support MI-1) and PW ≈ <PMo ≪ SiMo

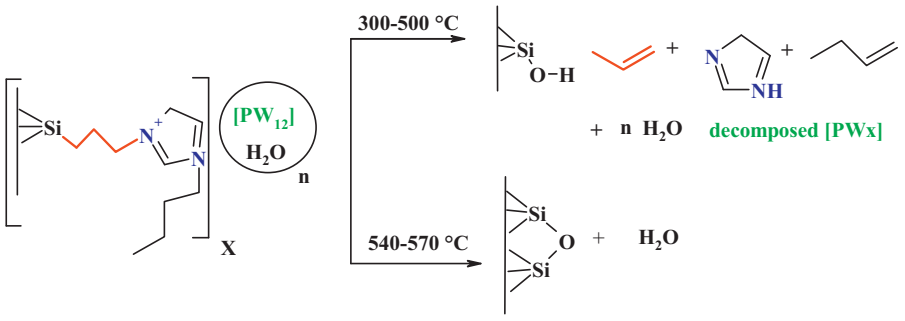

Scheme 2. Thermal decomposition of the salt of grafted N-propyl-N′-butylimidazolium cation with $H_3PW_{12}O_{40}$ acid.

(support BI-1). The most upfield TEPO chemical shifts and, respectively, the greatest acid site strength were observed for the immobilized tetrabasic acids $H_4SiW_{12}O_{40}$ and $H_4SiMo_{12}O_{40}$. These salts are likely to have the greatest number of acid protons. The ratio of the relative intensities of the ^{31}P SPE-MAS NMR peaks of TEPO adsorbed on acid centres (peak at 70–110 ppm) to those due to the Keggin anion allows us to estimate the number of TEPO molecules associated with one Keggin unit. This value is equal to number of acidic protons per KU available for interaction with TEPO (*ca.* 0.3–1).

4. Conclusion

In conclusion, we have developed a new method for preparing grafted onium salts of Keggin heteropolyacids ($H_3PMo_{12}O_{40}$, $H_3PW_{12}O_{40}$, $H_4SiMo_{12}O_{40}$·and $H_4SiW_{12}O_{40}$) via electrostatic immobilization on amorphous silica functionalized with pyridinium and alkylimidazolium cations.

The anion exchange of HPAs with onium-grafted silica results in solids where the Keggin structure of HPA anions is mostly intact. Immobilization of the molybdenum-based acid, $H_3PMo_{12}O_{40}$, is accompanied by the formation of some lacunary anions (up to *ca.* 5%).

The resulting materials have high dispersion of HPA over the surface, presumably as a monoanionic layer, and high surface areas and pore volumes, while no crystalline HPA can be detected by XRD.

These materials exhibit better resistance to HPA leaching than the silica-based materials. The greatest hydrolytic stability is displayed by $H_4SiW_{12}O_{40}$ and the worst by $H_3PMo_{12}O_{40}$-based catalysts. The solids demonstrate moderate thermal stability, depending on the onium cation and anion, in the range of 250–300 °C that is adequate for their use as catalysts. The thermal stability of the Keggin structure of the immobilized HPAs increases in the following order (T of disturbance of the Keggin structure): $H_3PMo_{12}O_{40}$ (200–250 °C) < $H_3PW_{12}O_{40}$ (300–350 °C) < $H_4SiW_{12}O_{40}$ (>350 °C). The stabilities of the salts run parallel to those of the parent acids (decomposition temperature):

$$SiO_2\text{–}Py_3PMo_{12}O_{40}(\approx 280\,^\circ C) \ll SiO_2\text{–}Py_3PW_{12}O_{40}(395\,^\circ C)$$

$$\leq SiO_2\text{–}Py_4SiW_{12}O_{40}(410\,^\circ C).$$

Peculiarities of the interaction between HPA and the surface–grafted cations afford acid salts. For this reason, these solids proved to be active heterogeneous catalysts in acid-catalysed reactions demanding moderate acidity [1].

The authors would like to express their gratitude to Professor Valeriy Karmanov, now deceased from cancer, who performed all measurements of W and Mo concentration by X-ray fluorescence technique.

References

[1] T.V. Kovalchuk, J.N. Kochkin, H. Sfihi, V.N. Zaitsev, J. Fraissard, J. Catal. 263 (2009) 247.
[2] T. Okuhara, T. Nakato, Catal. Surv. Jpn. 2 (1998) 31.
[3] N. Mizuno, M. Misono, Chem. Rev. 98 (1998) 199.
[4] A. Corma, Chem. Rev. 95 (1995) 559.
[5] M. Misono, Chem. Commun. (2001) 1141.
[6] A. Stein, M. Fendorf, T.P. Jarvie, Chem. Mater. 7 (1995) 304.
[7] G.G. Janauer, A. Dobley, J. Guo, P. Zavalij, M.S. Wittingham, Chem. Mater. 8 (1996) 2096.
[8] A. Taguchi, T. Abe, M. Iwamoto, Microporous Mesoporous Mater. 21 (1988) 387.
[9] M. Fournier, R. Thouvenot, C. Rocchiccioli-Deltcheff, J. Chem. Soc., Faraday. Trans. 87 (1991) 349.
[10] S. Shikata, T. Okuhara, M. Misono, J. Mol. Catal. A: Chem. 100 (1995) 49.
[11] N. Essayem, G. Coudurier, M. Fournier, J. Vedrine, Catal. Lett. 34 (1995) 223.
[12] V.N. Zaitsev, T.V. Kovalchuk, J. Fraissard, Functionalized Materials 2002, Kiev, Ukraine, 2002, p. 118;
T.V. Kovalchuk, V.N. Zaitsev, P. Batamack, H. Sfihi, J. Fraissard, Silica 2001, September 2001, Mulhouse, France, 2001;
T.V. Kovalchuk, V.N. Zaitsev, J. Fraissard, 4th Symposium "Supported Reagents and Catalysts in Chemistry", St. Andrews, UK, July, 2000, p. 40.
[13] M. Kamada, H. Kominami, Y. Kera, J. Colloid Interface Sci. 182 (1996) 297.
[14] M. Kamada, H. Nishijima, Y. Kera, Bull. Chem. Soc. Jpn. 66 (1993) 3565.
[15] Y. Kera, M. Kamada, Y. Hanada, H. Kominami, Compos. Interfaces 8 (2001) 109.
[16] T. Kovalchuk, H. Sfihi, V. Zaitsev, J. Fraissard, J. Catal. 249 (2007) 1.
[17] T.M. Jyothi, M.L. Kaliya, M. Herskowitz, M.V. Landau, Chem. Commun. 11 (2001) 992.
[18] M.H. Valkenberg, C. de Caestro, W.F. Hoelderich, 4th Symposium "Supported Reagents and Catalysts in Chemistry", St. Andrews, UK July, 2000, pp. 242–247.
[19] T. Kovalchuk, H. Sfihi, L. Kostenko, J. Fraissard, V. Zaitsev, J. Colloid Interface Sci. 302 (2006) 214.
[20] P. Tundo, P. Venturello, E. Angeletti, J. Am. Chem. Soc. 104 (1982) 6547.
[21] P. Tundo, P. Venturello, J. Am. Chem. Soc. 101 (1979) 6606.
[22] A. Kwon, T.J. Pinnavaia, J. Mol. Catal. 74 (1992) 23.
[23] L.A. Combs-Walker, C.L. Hill, Inorg. Chem. 30 (1991) 4016.
[24] I.V. Kozhevnikov, K.R. Kloetstra, A. Sinnema, H.W. Zandbergen, H. van Bekkum, J. Mol. Catal. A: Chem. 114 (1996) 287.
[25] I.V. Kozhevnikov, Catal. Rev. Sci. Eng. 37 (1995) 311.
[26] K. Bruckman, M. Che, J. Haber, J.M. Tatibouet, Catal. Lett. 25 (1994) 225.
[27] A. Ghanbari-Siahkali, A. Philippou, J. Dwyer, M.W. Anderson, Appl. Catal. A: Gen. 192 (2000) 57.
[28] V.M. Mastikhin, S.M. Kulikov, A.V. Nosov, I.V. Kozhevnikov, I.L. Mudrakowsky, M.N. Timofeeva, J. Mol. Catal. 60 (1990) 65.
[29] G. Baronetti, L. Briand, U. Sedran, H. Thomas, Appl. Catal. A: Gen. 172 (1998) 265.
[30] M. Fournier, C. Louis, M. Che, P. Chaque, D. Masure, J. Catal. 119 (1989) 400.
[31] N. Essayem, A. Holmquist, G. Sapaly, J.C. Vedrine, Y. Ben-Taarit, Stud. Surf. Sci. Catal. 135 (2001) 340.
[32] N. Essayem, S. Kieger, G. Coudurier, J.C. Vedrine, Stud. Surf. Sci. Catal. 101 (1996) 591.